한국수소 및 신에너지학회 논문집(2010. 4), 제21권 제2호
Trans. of the Korean Hydrogen and New Energy Society(2010. 4), Vol. 21, No. 2, pp. 89~97

니켈 기반 혼합 산화물의 수소 환원 특성: TPR 및 XRD 연구

류재춘*, 차광서*, 이동희*, 이영석*, 박주식, 김영호*†**
*충남대학교 정밀응용화학과, **한국에너지기술 연구원

Hydrogen Reduction Characteristics of Ni-based Mixed Oxides: TPR and XRD Study

JAECHUN RYU*, KWANGSEO CHA*, DONGHEE LEE*, YOUNGSEAK LEE*, CHUSIK PARK, YOUNGHO KIM*†**
**Department of Fine Chemical Engineering and Applied Chemistry, Chungnam National Univ., Daejeon 305-764, Korea*
***Korea Institute of Energy Research, 71-2 Jang-dong, Yuseoung-gu, Daejeon 305-343, Korea*

ABSTRACT

Al_2O_3, TiO_2, ZrO_2, Al_2O_3-TiO_2, Al_2O_3-ZrO_2 및 TiO_2-ZrO_2, 혼합 산화물을 지지체로 한 Ni 기반 혼합 산화물을 졸-겔법으로 제조하였다. 제조된 혼합 산화물은 1173K에서 열처리 한 후 구조적 특성 변화를 전자현미경 및 X-선 회절 분석을 이용하여 관찰하였으며, 수소를 이용한 승온 환원(TPR; temperature-programmed reduction) 실험을 통하여 1173K 까지 각 시료들의 환원 피크를 비교 고찰하였다. Al_2O_3 또는 TiO_2 가 혼합된 시료의 경우 1173K 에서의 열처리 후 니켈 알루미네이트 또는 니켈 티타네이트와 같은 새로운 결정상의 생성이 관찰되었으나 ZrO_2가 혼합된 경우에는 새로운 결정상의 생성이 관찰되지 않았다. TPR 결과에 의하면, Al_2O_3 또는 TiO_2를 혼합된 시료의 경우 벌크 NiO의 TPR 결과와는 달리 생성된 새로운 결정상에 기인한 여러 개의 환원 피크가 나타났으나 ZrO_2를 혼합한 경우 벌크 NiO와 비슷한 환원 피크를 보였다. TPR 결과를 기초로 Arrhenius plot 으로부터 각 혼합 산화물들의 수소 환원 활성화 에너지를 도출하였다. ZrO_2를 지지체로 사용하는 경우 다른 혼합 산화물들보다 지지체로서 안정한 혼합 산화물 상을 형성한다는 것을 지시하듯이 상대적으로 가장 낮은 활성화 에너지를 나타냈다.

KEY WORDS : Ni-based oxides(니켈 기반 산화물), TPR(승온 환원), Hydrogen reduction(수소 환원), Activation energy(활성화 에너지), ZrO_2 support(ZrO_2 지지체)

1. INTRODUCTION

Ni-based mixed oxides have been extensively studied as a catalyst in steam and CO_2 reforming of methane[1-5], selective hydro-dehydrogenation[6,7], and production of synthesis gas[8,9], which are industrially important. Furthermore, the feasibility of Ni-based catalysts has recently been reported for the production of hydrogen by catalytic decomposition of methane[10,11]. On the other hand, it is

†Corresponding author : yh_kim@cnu.ac.kr
[접수일 : 2009.11.7 수정일 : 2010.2.1 게재확정일 : 2010.4.20]

necessary to import support material with high thermal stability for suppressing aggregation between Ni-based catalysts in high temperature[12-15]. Therefore, various metal oxides have been considered and investigated as supports, including Al_2O_3, TiO_2, ZrO_2 and CeO_2 which have good thermal stability, a large specific area and surface properties such as acidity or basicity[3,5,9,16]. It is well known that the activity of the catalyst depends mainly on the reducibility of the active metal, which can be affected by the interaction of NiO with support components[17]. Consequently, it is necessary to investigate the reduction behavior of Ni-based oxides mixed with various supports.

In this study, Ni-based mixed oxides, containing component oxides such as Al_2O_3, TiO_2, ZrO_2, Al_2O_3-TiO_2, Al_2O_3-ZrO_2 and TiO_2-ZrO_2, were prepared using the sol-gel method. The reduction behavior of the Ni-based mixed oxides was investigated through temperature-programmed reduction (TPR) to 1173K in association with structural characteristics through X-ray diffraction (XRD) analysis.

2. EXPERIMENTAL

2.1 Preparation of Ni-based mixed oxides

The Ni-based mixed oxides were prepared by the following modified sol-gel process. Nickel nitrate (Junsei, 97%) was used as a source of nickel oxide. Aluminum (Aldrich, 99%), titanium (Aldrich, 97%) and zirconium isopropoxide (Aldrich, 99%) were used as the precursors of Al_2O_3, TiO_2 and ZrO_2, respectively. Each precursor was hydrolyzed with a hydrochloric acid solution in order to obtain the transparent sol. The obtained sol was added to an aqueous solution of copper nitrate at room temperature. The mixture was heated to 313K, vigorously agitated for 1h, titrated with NaOH aqueous solution to adjust to pH=10~11, stirred for 3h, heated to 373K and maintained for 2h without any agitation. The precipitate was filtered and washed with distilled water several times to remove the residual sodium hydroxide. The obtained gel was dried in an oven at 383K for 24h. The resulting gel powders were calcined at 1173K for 3h. The composition of the Ni-based mixed oxides was determined on the basis of the molar ratio of the final component oxides and the molar ratios of each component oxide were fixed to be equal.

2.2 Characterization

The TPR measurements were carried out using the apparatus described elsewhere[18]. The water evolved during the reduction was removed by a cooling trap, which was equipped in a gas line prior to the thermal conductivity detector. The temperature of the reactor was linearly raised at the desired rates by electrical furnace. The hydrogen-argon mixture (5% H_2/95% Ar) was used to reduce the samples at a flow rate of $40ml \cdot min^{-1}$. The prepared powders were sieved to be the range of 150~180μm before TPR measurement. Samples of 0.03g were mounted on a bed of tubular quartz reactor and reduced by hydrogen as the temperature was increased to 1173K at a heating rate in the range of 6 to $24K \cdot min^{-1}$. The experimental setup was depicted in Fig. 1. The mixed oxides underwent structural characterization by powder XRD technique using a Rigaku (D/max III-B) diffractometer (Ni-filtered Cu Kα). X-ray patterns were recorded from 10 to 70 degree (2Θ) at 40kV and 30mA. Scanning electron microscopy (SEM) images of the surface of the mixed oxides were obtained by gold coating method using JEOL equipment (JSM-6700F).

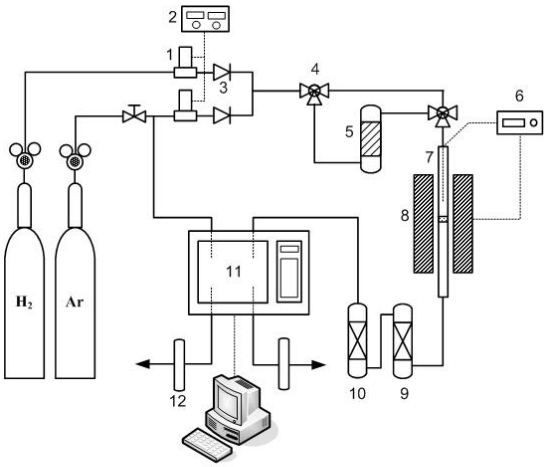

Fig. 1 Schematic diagram of experimental setup for TPR analysis.

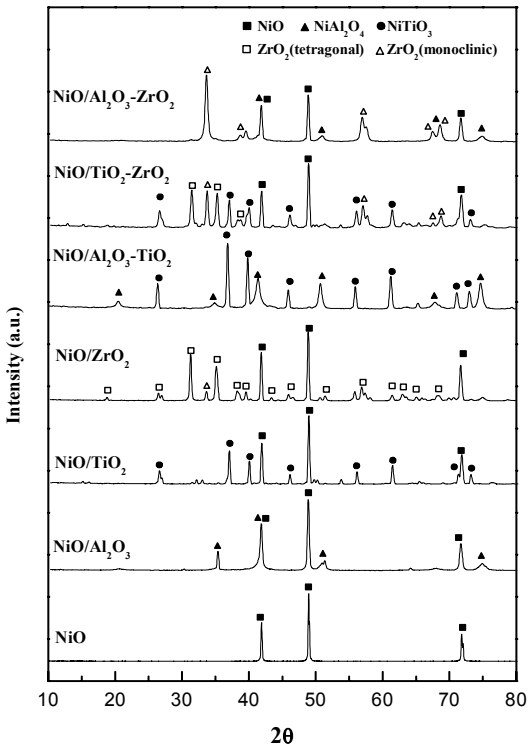

Fig. 2 X-ray diffraction patterns of the Ni-based mixed oxides calcined at 1173K.

3. RESULTS AND DISCUSSION

3.1 Characterization of mixed oxides

XRD patterns of mixed oxides are shown in Fig. 2. The main crystalline phases of the samples calcined at 1173K are also summarized in Table 1. As shown in Fig. 2 and Table 1, the diffraction patterns for the NiO samples clearly exhibited the characteristic peaks of nickel oxide with rhombohedral structure.

The XRD patterns of the NiO/Al_2O_3, NiO/Al_2O_3-TiO_2 and NiO/Al_2O_3-ZrO_2 samples which were mixed with Al_2O_3, showed the formation of $NiAl_2O_4$ crystallite, while those of the NiO/TiO_2, NiO/Al_2O_3-TiO_2 and NiO/TiO_2-ZrO_2 samples, which contained TiO_2, showed the formation of $NiTiO_3$ crystallite. These results were due to the solid-solid reaction of NiO and Al_2O_3 or TiO_2 by calcination at 1173K. It is well known that some metal oxides such as Ni, Co and Cu react with Al_2O_3 or TiO_2 to form new crystallites such as aluminates or titanates at

Table 1 Main crystalline phases of the Ni-based mixed oxides

Sample	Main phases	JCPDS File No.
NiO	NiO (rhombohedral)	44-1159
NiO/Al_2O_3	NiO (rhombohedral)	44-1159
	$NiAl_2O_4$ (cubic)	10-0339
NiO/TiO_2	NiO (rhombohedral)	44-1159
	$NiTiO_3$ (rhombohedral)	33-0960
NiO/ZrO_2	NiO (monoclinic)	44-1159
	ZrO_2 (monoclinic)	24-1165
	ZrO_2 (tetragonal)	17-0923
NiO/Al_2O_3-TiO_2	$NiAl_2O_4$ (cubic)	10-0339
	$NiTiO_3$ (rhombohedral)	33-0960
NiO/TiO_2-ZrO_2	NiO (rhombohedral)	44-1159
	$NiTiO_3$ (rhombohedral)	33-0960
	ZrO_2 (monoclinic)	24-1165
	ZrO_2 (tetragonal)	17-0923
NiO/Al_2O_3-ZrO_2	NiO (rhombohedral)	44-1159
	$NiAl_2O_4$ (cubic)	10-0339
	ZrO_2 (tetragonal)	17-0923

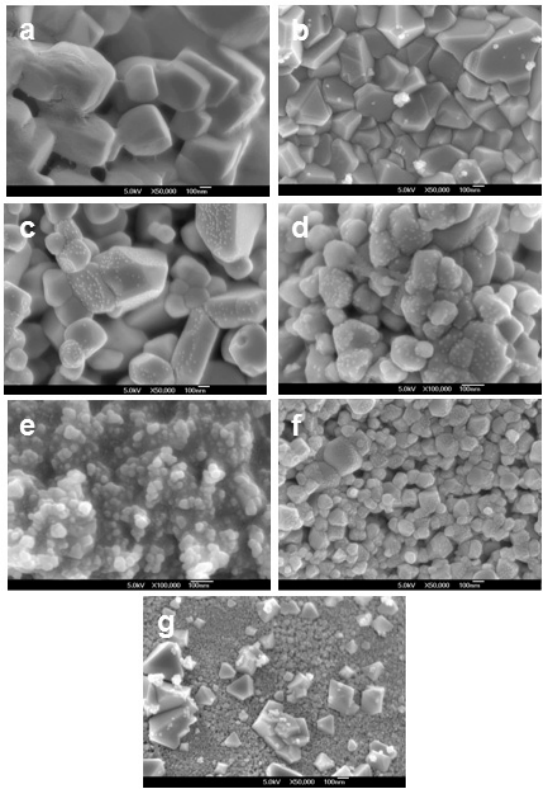

Fig. 3 SEM images of the Ni-based mixed oxides calcined at 1173K; (a) NiO, (b) NiO/Al_2O_3, (c) NiO/TiO_2, (d) NiO/ZrO_2, (e) NiO/Al_2O_3-TiO_2, (f) NiO/TiO_2-ZrO_2, and (g) NiO/Al_2O_3-ZrO_2.

high temperature. Such new crystallite formation can affect the redox property and activity of the mixed oxide when it is applied at high temperature.

On the other hand, the NiO/ZrO_2, NiO/TiO_2-ZrO_2 and NiO/Al_2O_3-ZrO_2 samples, which were mixed with ZrO_2, had a coexistent phase of NiO and ZrO_2 crystallite without any formation of new crystallite such as zirconates. This result suggested that the reduction behaviors of the mixed oxides mixed with Al_2O_3 or TiO_2 are different from that of bulk NiO.

Fig. 3 presents the SEM images of the mixed oxides. As shown in Fig. 3(a), the SEM image of bulk NiO showed large NiO particles with a grain size of several hundred nanometers due to calcination at the high temperature of 1173K. The SEM images of the samples mixed with Al_2O_3 or TiO_2 (Fig. 3(b) and (c)) also showed large particles with well developed crystal faces which were attributed to bulk NiO and $NiAl_2O_4$ or $NiTiO_3$. Such morphologies were partially found in the NiO/TiO_2-ZrO_2 and NiO/Al_2O_3-ZrO_2 samples (Fig. 3(f) and (g)) due to $NiTiO_3$ and $NiAl_2O_4$, respectively, whereas for the NiO/Al_2O_3-TiO_2 sample (Fig. 3(e)), which had $NiAl_2O_4$ and $NiTiO_3$ crystallites without any formation of bulk NiO crystallites as evidenced by the XRD result, an intermediate state between small $NiAl_2O_4$ and $NiTiO_3$ particles was observed and no separated phases of bulk nickel oxides were found. The samples mixed with ZrO_2 (Fig. 3(d)) mainly exhibited the morphology of typical ZrO_2 particles rather than bulk NiO particles, suggesting that bulk NiO particles were buried in the ZrO_2 particles.

3.2 H_2-TPR study

The H_2-TPR patterns of the Ni-based mixed oxides, which were obtained by heating to 1173K at a rate of $12K \cdot min^{-1}$, are displayed in Fig. 4 in comparison with that of bulk NiO. As shown in Fig. 4(a), the TPR pattern of bulk NiO consisted of one broad peak in the range of ca. 600 to 950K with a maximum peak at 682K. It has been reported in previous works that the TPR pattern of bulk NiO has a maximum peak at 600K ($4.5K \cdot min^{-1}$) or 691K ($10K \cdot min^{-1}$) due to reduction of $Ni^{2+} \rightarrow Ni^0$ course[19,20]. The results in the present study were in good agreement with the previous works. To explain the marked decrease in the reduction rate after the maximum peak, we examined the nucleation growth model that has been proposed for the reduction mechanism of bulk NiO[18]. Bulk NiO is rapidly reduced by hydrogen

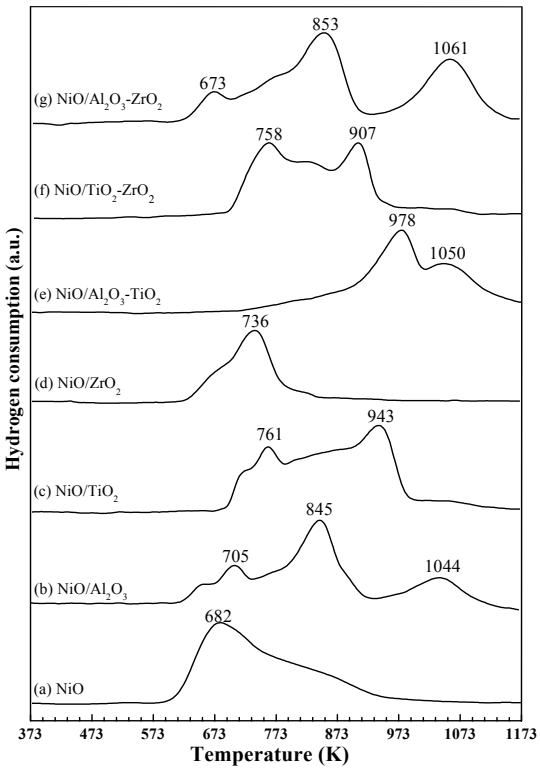

Fig. 4 TPR profiles of the Ni-based mixed oxides; Sample weight = 30mg, heating rate = 12K·min^{-1}, reducing gas = 5% H_2/95% Ar, and gas flow rate = 40ml·min^{-1}.

at the initial stage to form metal nuclei at the surface of the oxide. With increasing reaction interface, the metal nuclei grow and decrease the reaction rate due to the overlapping of the metal nuclei. Therefore, the decreased reduction rate after the maximum peak was attributed to this reduction mechanism.

As shown in Fig. 4(b), the H_2-TPR profile of the NiO/Al_2O_3 sample was different from that of the bulk NiO sample. The TPR patterns of NiO/Al_2O_3 showed complicated and broad peaks in the range of about 693~1073K, with three maximum peaks at 705, 845 and 1044K. These results indicated that the H_2 reduction proceeded through the multi-stages. Many publications have previously reported on the TPR results of nickel oxide catalysts supported by alumina using the impregnation or co-precipitation method. In these previous works, several reduction peaks were observed in the TPR profiles of the supported NiO. Low temperature peaks are generally attributed to the reduction of larger NiO particles which are similar in nature to pure bulk NiO, while the high temperature peaks are attributed to the reduction of NiO with intimate contact with the oxide support[21]. Consequently, the maximum peak at 705 and 845K was possibly due to the reduction of bulk NiO and the reduction of Ni-O-Al bond which was formed by a weak interaction between bulk NiO and Al_2O_3, respectively. The peak at 1044K is attributed to the reduction of $NiAl_2O_4$ crystallite. The NiO/TiO_2 mixed oxide showed the maximum peaks at 761K and 943K (Fig. 4(c)), possibly due to the reduction of bulk NiO and $NiTiO_3$, respectively.

On the other hand, the TPR pattern of NiO/ZrO_2 in Fig. 4(d) showed one peak at about 736K, indicating that only one reduction step through $Ni^{2+} \rightarrow Ni^0$ occurred. The peak shape of NiO/ZrO_2 was different from that of bulk NiO. As mentioned above, bulk NiO showed a reduction peak according to the nucleation growth model in which the reaction rate proceeded rapidly in the initial stage but decreased in the final stage of reduction. However, the results indicated that the H_2-reduction of NiO/ZrO_2 did not proceed similarly to that of bulk NiO.

Fig. 4(e)~(g) shows the H_2-TPR patterns of the Ni-based ternary oxides with Al_2O_3-TiO_2, Al_2O_3-ZrO_2 and TiO_2-ZrO_2. As shown in Fig. 4(e), the pattern of NiO/Al_2O_3-TiO_2 consists of two maximum peaks at 978 and 1050K. As compared with the TPR patterns in Fig. 4(b) and (c), the two peaks are due to the reduction of $NiTiO_3$ and $NiAl_2O_4$, respectively. Similarly, the reduction peaks of NiO/TiO_2-ZrO_2 (Fig. 4(f)) at 758 and 907K were attri-

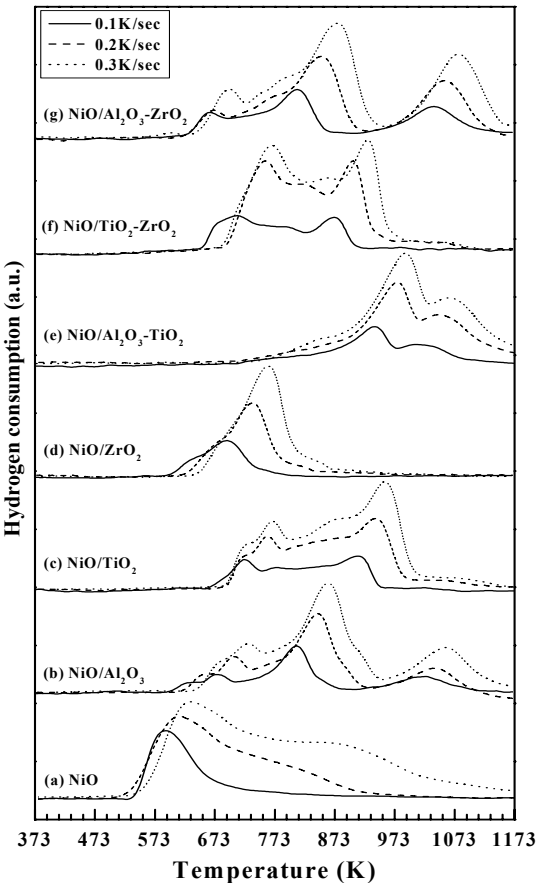

Fig. 5 Variation of TPR patterns of the Ni-based mixed oxides with increasing heating rate.

buted to the reduction of bulk NiO and $NiTiO_3$, respectively. The TPR patterns of NiO/Al_2O_3-ZrO_2 (Fig. 4(g)) can be interpreted as follows: a peak at 673K due to the reduction of the Ni-O bond in bulk NiO and two peaks at 853 and 1061K due to the reduction of Ni-O in the form of the weak and strong Ni-O-Al bond in the $NiAl_2O_4$ crystallite, respectively.

3.3 Activation energy of H_2 reduction

In order to extract the kinetic parameter from the TPR experiment, Wimmers et al.[22] have reported a convenient method expanding Kissinger's approach

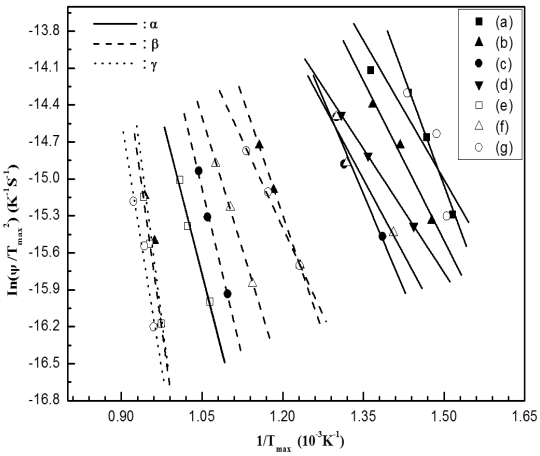

Fig. 6 Temperature-programmed Arrhenius plots obtained from TPR data of the Ni-based mixed oxides; (a) NiO, (b) Ni/Al_2O_3, (c) NiO/TiO_2, (d) NiO/ZrO_2, (e) NiO/Al_2O_3-TiO_2, (f) NiO/TiO_2-ZrO_2, and (g) NiO/Al_2O_3-ZrO_2.

to obtain the apparent activation energy from differential thermal analysis data. From Wimmers's method, the activation energy can be calculated from the TPR data by the following equation:

$$\ln\left(\frac{\Psi}{T_{\max}^2}\right)=\frac{-E_a}{RT_{\max}}+\ln\left(\frac{AR}{E_a}\right)+C$$

The activation energy (E_a) is obtained from the shift of the rate of maximum temperature (T_{max}) against heating rate (Ψ). If the plot of $\ln(\Psi/T_{max}^2)$ versus $1/(T_{max})$ results in a straight line, the slope of the plot is E_a/R, where R is the gas constant. The conversion at T_{max} is assumed to be independent of the heating rate. In the variation of the TPR patterns of the mixed oxides with increasing heating rate (Fig. 5), the rate maximum temperature was shifted to a higher temperature with increasing heating rate. Fig. 6 shows the temperature programmed "Arrhenius plots" according to Wimmers's approach, as described above. The plots of $\ln(\Psi/T_{max}^2)$ versus $1/(T_{max})$ were all fitted in a straight line. The activation energies of the mixed oxides

Table 2 Activation energies for the H_2 reduction of Ni-based mixed oxides calculated from temperature programmed Arrhenius plots

Sample	Peaks	Activation energy (kJ/mol)
NiO	α	62.7
NiO/Al_2O_3	α	71.9
	β	106.3
	γ	281.0
NiO/TiO_2	α	85.4
	β	151.7
NiO/ZrO_2	α	55.3
NiO/Al_2O_3-TiO_2	α	141.0
	β	142.3
NiO/TiO_2-ZrO_2	α	68.0
	β	118.5
NiO/Al_2O_3-ZrO_2	α	99.0
	β	78.6
	γ	223.3

for H_2 reduction were calculated from the slope of the plot and are listed in Table 2, where α, β and γ denote the peaks in order from low to high temperature, respectively. The activation energy of bulk NiO was ca. 63kJ·mol^{-1}. In the case of the NiO/ZrO_2 sample, the activation energy due to the reduction of bulk NiO was analogous to that of bulk NiO, suggesting that the ZrO_2 was a stable support for hydrogen reduction. However, the NiO/TiO_2 and NiO/Al_2O_3 samples needed a higher activation energy than that of bulk NiO, indicating that the nickel oxide contained in the NiO/TiO_2 and NiO/Al_2O_3 samples is difficult to be reduced because of Ni-O-Ti or Ni-O-Al bond.

4. CONCLUSION

Ni-based mixed oxides were prepared by sol-gel method and their reduction properties and structural characteristics were investigated by the TPR technique and XRD analysis, respectively. From the results, the following conclusions were drawn.

1) Ni-based oxides mixed with Al_2O_3 or TiO_2 showed the formation of new crystallites such as nickel aluminates or titanates through calcination at 1173K. Meanwhile, the crystalline structure of Ni-based oxides mixed with ZrO_2 showed as simple mixing phase of component oxides without any new crystallite formation.
2) The TPR patterns of Ni-based oxides mixed with Al_2O_3 or TiO_2 consisted of multi-peaks and showed different reduction behaviors than that of bulk NiO due to the reduction of new crystallites such as aluminates or titanates, whereas the TPR patterns of Ni-based oxides mixed with ZrO_2 consisted of one peak and were similar to that of bulk NiO.
3) The activation energy of Ni-based mixed oxides was calculated by Arrhenius plots from the TPR data. The results indicated that compared to bulk NiO, Ni-based oxides mixed with Al_2O_3 or TiO_2 need higher activation energies to reduce all the Ni species due to the formation of aluminates or titanates. Meanwhile, the activation energy of a NiO/ZrO_2 sample was slightly lower than that of bulk NiO, suggesting that the ZrO_2 was a stable support for hydrogen reduction.

ACKNOWLEDGMENT

This research was performed for the Hydrogen Energy R&D Center, one of the 21st Century Frontier R&D Program, funded by the Ministry of Education, Science and Technology of Korea.

REFERENCES

1) J. T. Richardson, R. M. Scates, and M. V. Twigg: "X-ray diffraction study of the hydrogen reduction of NiO/α-Al_2O_3 steam reforming catalysts", Appl. Catal., A., Vol. 267, No. 1-2, 2004, pp. 35-46.
2) J. M. Wei, B. Q. Xu, J. L. Li, Z. X. Cheng,

and Q. M. Zhu: "Highly active and stable Ni/ZrO_2 catalyst for syngas production by CO_2 reforming of methane", Appl. Catal., A., Vol. 196, No. 2, 2000, pp. L167-L172.

3) V. R. Choudhary, S. Banerjee, and A. M. Rajput: "Hydrogen from step-wise steam reforming of methane over Ni/ZrO_2: factors affecting catalytic methane decomposition and gasification by steam of carbon formed on the catalyst", Appl. Catal., A., Vol. 234, No. 1-2, 2002, pp. 259-270.

4) H. S. Roh, K. W. Jun, and S. E. Park: "Methane-reforming reactions over Ni/Ce-ZrO_2/Θ-Al_2O_3 catalysts", Appl. Catal., A., Vol. 251, No. 2, 2003, pp. 275-283.

5) S. Wang and G. Q. Lu: "Role of CeO_2 in Ni/CeO_2-Al_2O_3 catalysts for carbon dioxide reforming of methane", Appl. Catal., B., Vol. 19, No. 3-4, 1998, pp. 267-277.

6) C. Guimon, A. Auroux, E. Romero, and A. Monzon: "Acetylene hydrogenation over Ni-Si-Al mixed oxides prepared by sol-gel technique", Appl. Catal., A., Vol. 251, No. 1, 2003, pp. 199-214.

7) E. Heracleus, A. F. Lee, K. Wilson, and A. A. Lemonidou: "Investigation of Ni-based alumina-supported catalysts for the oxidative dehydrogenation of ethane to ethylene: structural characterization and reactivity studies", J. Catal., Vol. 231, No. 1, 2005, pp. 159-171.

8) D. Dissanayake, M. P. Rosynek, K. C. C. Kharas, and J. H. Lunsford: "Partial oxidation of methane to carbon monoxide and hydrogen over a Ni/Al_2O_3 catalyst", J. Catal., Vol. 132, No. 1, 1991, pp. 117-127.

9) Q. G. Yan, W. Z. Weng, H. L. Wan, H. Toghiani, R. K. Toghiani, and C. U. Pittman: "Activation of methane to syngas over a Ni/TiO_2 catalyst", Appl. Catal., A., Vol. 239, No. 1-2, 2003, pp. 43-58.

10) I. Suelves, M. J. Lazaro, R. Moliner, B. M. Corella, and J. M. Palacios: "Hydrogen production by thermo catalytic decomposition of methane on Ni-based catalysts: influence of operating conditions on catalyst deactivation and carbon characteristics", Int. J. Hydrogen Energy., Vol. 30, No. 15, 2005, pp. 1555-1567.

11) S. Takenaka, H. Ogihara, I. Yamanaka, and K. Otsuka: "Decomposition of methane over supported-Ni catalysts: effects of the supports on the catalytic lifetime", Appl. Catal., A., Vol. 217, No. 1-2, 2001, pp. 101-110.

12) 류재춘, 김영호, 박주식, 황갑진, 김종원: "MO/Al_2O_3-ZrO_2 (M=Ni 및 Cu) 혼합 금속 산화물의 환원-산화 특성", 한국수소 및 신에너지학회 논문집, Vol. 16, No. 1, 2005, pp. 49-57.

13) 차광서, 류재춘, 이동희, 김영호, 박주식, 김종원: "ZrO_2 첨가 MnO_2/Mn_2O_3/NaOH 계를 이용한 열화학적 물분해 수소제조 실험 연구", 한국수소 및 신에너지학회 논문집, Vol. 17, No. 4, 2006, pp. 353-361.

14) 차광서, 이동희, 조원준, 이영석, 김영호: "페라이트계 금속 산화물 매체 상에서 열화학 메탄 개질 반응 특성", 한국수소 및 신에너지학회 논문집, Vol. 18, No. 2, 2007, pp. 140-150.

15) 이동희, 김홍순, 차광서, 박주식, 강경수, 김영호: "열화학 수소 제조를 위한 금속 치환 페라이트 매체의 부분 환원 및 물 분해 특성", 한국수소 및 신에너지학회 논문집, Vol. 18, No. 4, 2007, pp. 356-364.

16) O. Dewaele and G. F. Froment: "TAP Study of the Mechanism and Kinetics of the Adsorption and Combustion of Methane on Ni/Al_2O_3 and NiO/Al_2O_3", J. Catal., Vol. 184, No. 2, 1999, pp. 499-513.

17) H. M. Swaan, V. C. H. Kroll, G. A. Martin, and C. Mirodatos: "Deactivation of supported nickel catalysts during the reforming of methane by carbon dioxide", Catal. Today, Vol. 21, No.

2-3, 1994, pp. 571-578.

18) N. W. Hurst, S. J. Gentry, A. Jones, and B. D. McNicol: "Temperature Programmed Reduction", Catal. Rev. - Sci. Eng., Vol. 24, No. 2, 1982, pp. 233-309.

19) S. D. Robertson, B. D. McNicol, J. H. De Baas, S. C. Kloet, and J. W. Jenkins: "Determination of reducibility and identification of alloying in copper-nickel- on-silica catalysts by temperature-programmed reduction", J. Catal., Vol. 37, No. 3, 1975, pp. 424-431.

20) R. Brown, M. E. Cooper, and D. A. Whan: "Temperature programmed reduction of alumina-supported iron, cobalt and nickel bimetallic catalysts", Appl. Catal., Vol. 3, No. 2, 1982, pp. 177-186.

21) A. M. Diskin, R. H. Cunningham, and R. M. Ormerod: "The oxidative chemistry of methane over supported nickel catalysts", Catal. Today, Vol. 46, No. 2-3, 1998, pp. 147-154.

22) O. J. Wimmers, P. Arnoldy, and J. A. Moulijn: "Determination of the reduction mechanism by temperature-programmed reduction: application to small iron oxide (Fe_2O_3) particles", J. Phys. Chem., Vol. 90, No. 7, 1986, pp. 1331-1337.